# Improving DIC microscopy with polarization modulation

G. HOLZWARTH,* S. C. WEBB,* D. J. KUBINSKI† & N. S. ALLEN†
*Department of Physics, Wake Forest University, Winston-Salem, NC 27109, U.S.A.*
†Department of Botany, North Carolina State University, Raleigh, NC 27695, U.S.A.

## Summary

It is demonstrated experimentally, as well as analytically, that when the polarization of the light incident upon the first Nomarski–Wollaston prism in a differential interference contrast (DIC) light microscope is switched by 90°, image highlights are changed into shadows and vice versa. Using an inexpensive ferroelectric liquid-crystal modulator, which is easily installed in the microscope, this switching can be done at 30 frames s$^{-1}$, synchronized to the camera. Subtraction of alternate digitized frames generates a stream of images in which contrast is doubled, compared with conventional video-enhanced DIC, while image defects and noise tend to cancel. Subtraction of alternate images is carried out efficiently by frame buffer operations and amounts to massively parallel synchronous detection. The new method eliminates the problems inherent in obtaining a separate background image, as required by current video-enhanced DIC practice, without loss of resolution.

## Introduction

Differential interference contrast (DIC) light microscopy, particularly when coupled with digital image processing, is a powerful tool for the high-resolution microscopy of unstained biological specimens (Allen *et al.*, 1981; Inoué, 1981, 1986; Allen & Allen, 1983; Salmon, 1995). This paper shows that the contrast in such digitally enhanced DIC images can be increased by a factor of two by switching the polarization of the incident light by 90° in alternate frames with a ferroelectric liquid crystal modulator. Switching the polarization changes image highlights into shadows and vice versa. By subtracting alternate frames, a difference DIC image is created in which contrast is doubled while image defects and noise tend to cancel. The method can take full advantage of the extended dynamic range and more precise digitization of modern CCD cameras as well as the increased speed of modern frame processors. Because the modulator can be synchronized with frame acquisition

Correspondence to: G. Holzwarth

by the camera, electronic phase-sensitive detection can be carried out efficiently by frame buffer operations; a lock-in amplifier (Horowitz & Hill, 1989) is unnecessary. The need for a background image (Allen & Allen, 1983; Salmon, 1995), which requires some operator skill for best implementation, is eliminated.
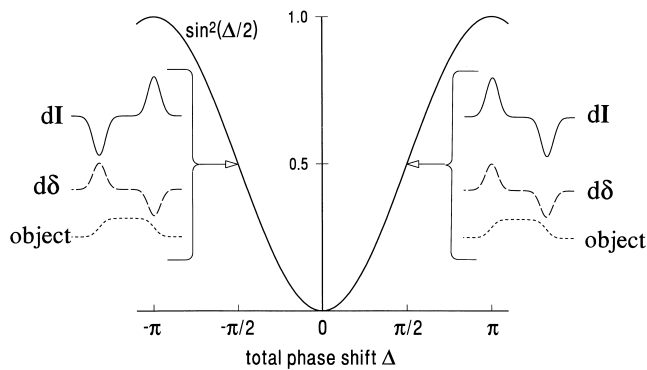
Optical phase modulation has been used previously in several scanning microscopes (Hansen *et al.*, 1985; Juang *et al.*, 1988; Mickols & Maestre, 1988). Image contrast in these instruments required that the sample be birefringent or dichroic, and employed one lock-in amplifier to carry out electronic phase-sensitive detection. Image generation was therefore slow. Recently, the ability of the polarization microscope to image weakly birefringent specimens was improved by replacing the standard compensator with two liquid-crystal modulators (Oldenbourg & Mei, 1995). Images based upon either the magnitude or the direction of the local birefringence are generated by digital manipulation of four images obtained with different settings of the two modulators. In our DIC method, image contrast arises from spatial gradients in refractive index, a more universal feature of biological structures, and frame buffer operations act like a massively parallel array of lock-in amplifiers.

## Materials and methods

A microscope fitted with DIC optics, a 75-W xenon source, an plan-apochromatic condenser (NA 1·4), and a 63× plan-apochromatic objective (NA 1·4), all manufactured by Zeiss, was used to test the polarization-modulation concept. Images were captured with a cooled CCD camera (1317×1035 pixels, 12-bit digitization, Princeton Instruments PentaMAX) under the control of Universal Imaging's Metamorph software. The polarizer and analyser were crossed; the transmission axis of the polarizer will be designated the *x*-direction.

A ferroelectric liquid-crystal modulator 5 mm thick with 25-mm-aperture (Displaytech) was installed into a swing-out holder which fitted between the polarizer and the condenser. This device acted as a half-wave plate whose fast

**Fig. 1.** Generation of image contrast in a DIC microscope with $x$-polarized and $y$-polarized light incident on the first Wollaston prism. The main curve shows the relative intensity $I/I_0 = \sin^2(\Delta/2)$ as a function of the total phase shift $\Delta = \Gamma + \delta$. The inset on the right corresponds to normal DIC with $x$-polarized light. The phase object shown has $\delta > 0$ on its left edge and $\delta < 0$ on its right edge. The offset $\Gamma$ is set to $+\pi/2$. This gives an 'operating point' on the right side of the null in the $\sin^2(\Delta/2)$ curve. As a consequence, $I > I_B$ on the left edge of the object, but $I < I_B$ on the right edge of the object, giving standard shading. The inset on the left describes what happens if the input light is $y$-polarized, but offset $\Gamma$ remains $\pi/2$ and the spatial dependence of $\delta$ caused by the sample is unchanged. Because of the change in polarization, the 'operating point' is now on the left side of the null in the $\sin^2(\Delta/2)$ curve, that is, $\Delta = -\pi + \Gamma + \delta$. Therefore, the intensity on the left edge of the object is less than the intensity at the right edge. This leads to inverted shading.

axis could be switched electrically by $45°$ in $35\,\mu s$. It was oriented in the microscope so that, in one of its two states, the wave plate fast axis was orientated parallel to $x$, the polarization direction of the light incident on the first Wollaston. When in the other state, the light transmitted by the waveplate was polarized along $y$. The electronic controller for the waveplate could be synchronized with the camera and could flip the polarization between $x$ and $y$ at frame rates. For the present demonstration, the modulator controller was set to a period of $4\,s$, while the camera acquired an image every $2\,s$. Typically, 16 images of the specimen were acquired in rapid sequence, with frames 0, 2, 4 ... having $x$-polarization and frames 1, 3, 5 ... having $y$-polarization. The modulator response time and electronics could readily support polarization modulation synchronized to a camera operating at 30 frames s$^{-1}$.

Computation of difference images was performed off-line with ImagePro 1.3 software because the available on-line image-processing speed was too slow. Images were printed from 8-bit files via Adobe Photoshop by a Fuji Pictrography 3000 printer. No image enhancements were carried out.

A diatom resolution test plate (Carolina Biological Supply B25D) was used to assess the performance of the microscope with and without polarization modulation.

### How polarization-modulation increases contrast

In conventional DIC microscopy (Lang, 1968; Allen *et al.*, 1969) light with intensity $I_0$ first traverses a linear polarizer, becoming $x$-polarized. A Nomarski–Wollaston prism then splits the beam into two beams polarized at $+45°$ and $-45°$ to the $x$-axis. The prism also introduces a slight spatial offset $ds$ between the two beams. As the two wavefronts travel through the sample, their relative phase is changed by an amount $\delta$. The value of $\delta$ varies from point to point in the wavefront and contains the information needed to create an image. After passing through the objective, the two beams pass through a second Nomarski–Wollaston prism, which has two functions. First, an additional phase shift, designated $\Gamma$ ('offset') can be introduced between the two wavefronts by manually moving the second prism from its central position. This gives a total phase shift $\Delta = \Gamma + \delta$ between the two beams. In addition, the spatial offset $ds$, imposed by the first prism, is removed by the second prism. The recombined beams are then caused to interfere by an analyser orientated to transmit $y$-polarized light, i.e. crossed with the polarizer.

The intensity of the light transmitted by the analyser is given by

$$I = I_0 \sin^2(\Delta/2) = I_0 \sin^2[(\Gamma + \delta)/2]. \tag{1}$$

A plot of $I/I_0$ against $\Delta$ is shown in Fig. 1. It has a minimum at $\Delta = 0$ and maxima at $\Delta = \pm\pi$. Note also that the slope of the curve has a maximum at $\Delta = \pi/2$ and a minimum, of equal amplitude, at $\Delta = -\pi/2$.

The image is generated by small intensity differences above and below background that arise from the phase shift $\delta$ created by the sample. The easiest way to evaluate these small intensity differences from Eq. (1) is to compute the differential $dI = (\partial I/\partial\delta)d\delta + (\partial I/\partial\Gamma)d\Gamma$. Within a given image, the offset $\Gamma$ is constant, so $d\Gamma$ is zero. Therefore,

$$dI = I_0 \sin(\Gamma/2)\cos(\Gamma/2)d\delta = (I_0/2)\sin\Gamma\,d\delta. \tag{2}$$

Now $\Gamma$ is normally set greater than zero, so that $\sin\Gamma > 0$ in Eq. (2). Thus, an embedded phase object within the sample will normally have a highlight ($dI > 0$) on its upper left edge and a shadow ($dI < 0$) at its lower right edge, as explained in Fig. 1, right-hand inset, This gives the apparent 3-D effect characteristic of DIC images (Lang, 1968; Allen *et al.*, 1969).

Switching the polarization of the incident light from $x$ to $y$ causes an additional phase shift of $-\pi$ in one of the two spatially offset beams which traverse the sample. The total phase shift in this beam relative to the other beam is thus $\Delta = -\pi + \Gamma + \delta$. The signal $dI$ arising from a small $d\delta$ is then

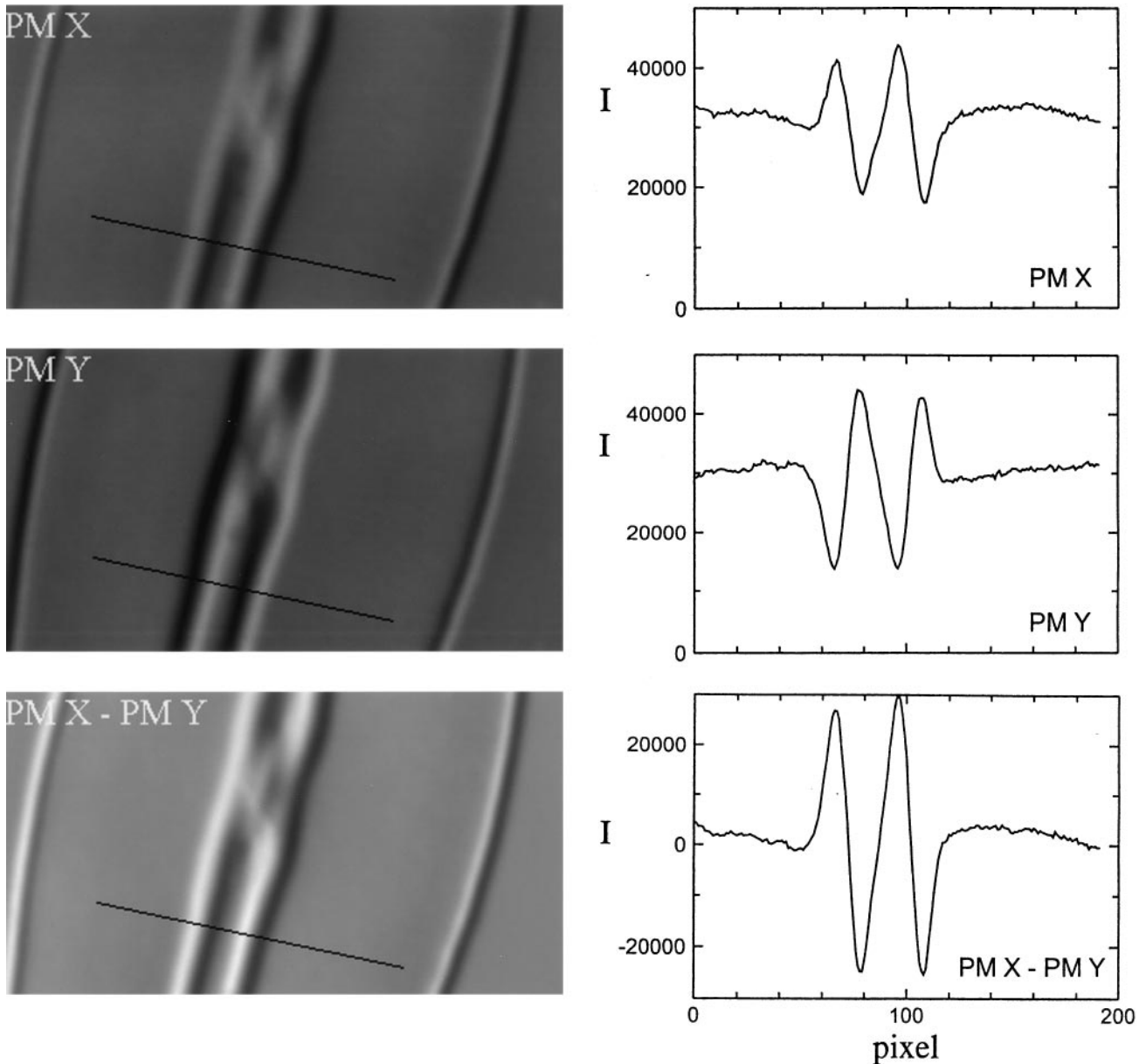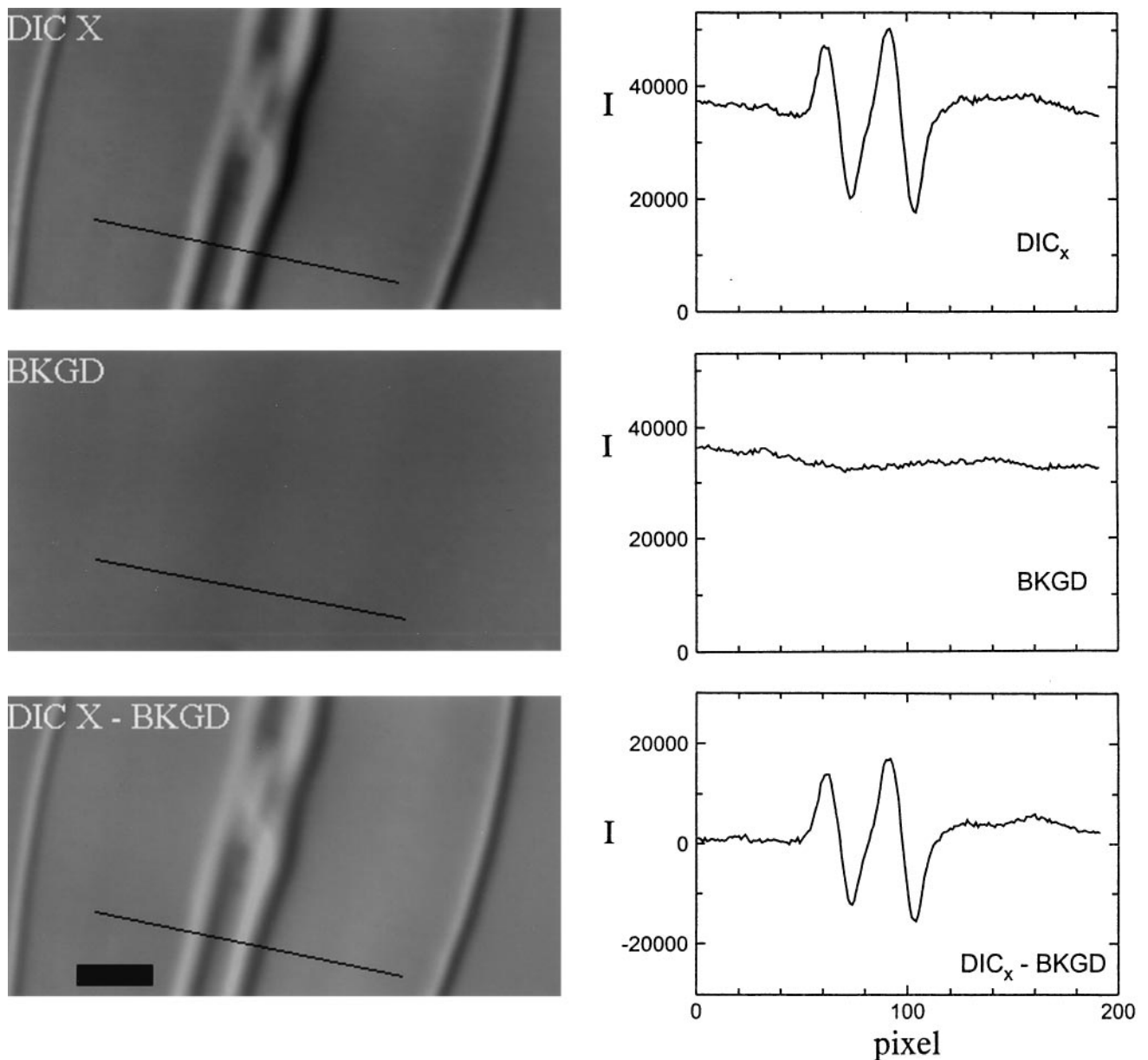$$dI = (I_0/2)\sin(-\pi + \Gamma)d\delta = -(I_0/2)\sin\Gamma\,d\delta. \tag{3}$$

**Fig. 2.** Images and linescans of a small region of the diatom *Frustulia rhomboides* obtained by polarization-modulated DIC microscopy. Left side (images): PM X: DIC image obtained with *x*-polarized incident light. PM Y: DIC image obtained with *y*-polarized incident light. PM X − PM Y: difference DIC image, obtained by subtracting PM Y from PM X, then adding 32 768 (middle of grey scale) to ensure that all intensities were greater than zero. The length of the linescan is 8·4 $\mu$m. Right side (linescans): the three graphs show the intensity along the line marked on the corresponding images to the left. For PM X − PM Y the linescan was determined before the zero of intensity was moved to the middle of the grey scale.

This is identical to Eq. (2), but with a minus sign. This means that those regions of the image which were highlights in *x*-polarized DIC become shadows in *y*-polarized DIC, and vice versa, as shown in the left-hand inset in Fig. 1.

If the image is to be viewed by eye, one must optimize image contrast $dI/I_B$ rather than $dI$ alone (Inoué, 1986). The background intensity is given by $I_B = I_0 \sin^2(\Gamma/2)$. In video- or digitally enhanced DIC, setting $\Gamma$ to approximately $\pi/2$ gives an operating point on the intensity curve, $I = I_0 \sin^2(\Delta/2)$, where the slope is a maximum. This maximizes $dI$. The concomitant undesirable increase in background intensity to $I_0/2$ is normally removed either by offsetting the camera's analog electronic zero (Allen *et al.*, 1981; Inoué, 1981) or by digitizing the image and subtracting from it a defocused or spatially shifted background image (Allen & Allen, 1983; Salmon, 1995). The resultant

**Fig. 3.** Images and linescans of a small region of the diatom *Frustulia rhomboides* obtained by video-enhanced DIC microscopy. Left side (images): DIC X: DIC image obtained with *x*-polarized incident light. BKGD: defocused DIC image obtained with *x*-polarized light. DIC X − BKGD: difference DIC image, obtained by subtracting the two images above, then adding 32 768, as in Fig. 2. Scale bar = 2·0 μm. Right side (linescans): the three graphs show the intensity along the line marked on the corresponding images to the left. For DIC X − BKGD, the linescan was determined before the zero of intensity was moved to the middle of the grey scale 32 768.

'video-enhanced' or 'digitally enhanced' image is then viewed on a high-resolution computer monitor, rather than directly through the oculars of the microscope. Our method improves upon this procedure by electro-optically switching the polarization of the light incident on the first Wollaston prism in alternate frames. When alternate frames are subtracted from one another, background is automatically cancelled out, while the values of d*I* in alternate frames reinforce one another.

*Experimental tests of contrast and resolution*

Digital images of the diatom *Frustulia rhomboides* were collected with polarization modulation. Images 0, 2, 4, etc., were obtained with *x*-polarization; images 1, 3, 5, etc., had *y*-polarization. The offset Γ was easily set to the desired value of $\pi/2$ by adjusting the position of the second Wollaston beam splitter until the even-numbered images had the same background intensity as the odd-numbered

images. The x-images had normal shadowing, whereas the y-images had reversed shadowing, as shown in Fig. 2, images PM X and PM Y. Both images showed the expected high background, which made visual contrast poor. However, when the y-image was subtracted from the x-image to create the difference image, the background was close to zero. The highlights in the difference image had peak numerical values of approximately +30 000. The shadows reached numerical values of about −30 000 in the frame buffer. Such negative numbers could not be displayed properly because the 16-bit grey scale had values between 0 and 65 535. To display the difference image properly therefore, the zero of the difference image was placed in the middle of the 16-bit grey scale by adding 32 768 to it. The improved contrast of the resultant difference image is shown in Fig. 2, bottom image, labelled PM X − PM Y.

To demonstrate quantitatively how the intensity at a given pixel changed when the polarization was modulated, linescans for identical paths within the three images are shown on the right side of Fig. 2. For both PM X and PM Y, the intensity oscillates between $\approx 15\,000$ and $45\,000$. However, the peaks in the linescan for PM X correspond to valleys in the linescan for PM Y, as expected from the sign reversal of d$I$ predicted by Eqs. (2) and (3). The linescan through the difference image showed the expected doubling of deviations from background compared with either PM X or PM Y (Fig. 2, right side, lowest graph), with peaks of $\approx 63\,000$ and shadows of $\approx 3000$.

As a control, standard x-polarized DIC images of the same region of the same diatom were acquired with the modulator swung out of the lightpath, keeping the offset $\Gamma$ unchanged at $\pi/2$. The resultant image is shown as DIC X in Fig. 3. The microscope was then defocused and a second image was obtained for use in background subtraction. The resultant image is shown as BKGD in Fig. 3. When the background image was subtracted from the x-polarized DIC image and offset to the middle of the grey scale, the third image, DIC X − BKGD, was obtained; this corresponds to standard video-enhanced DIC (Allen & Allen, 1983; Salmon, 1995). Linescans for DIC X, BKGD and the difference image are shown on the right side of Fig. 3. The peak-to-peak amplitude of the intensity oscillations in the difference image (DIC X − BKGD) were only half as large as those generated by the polarization-modulation method, because the background image was, as expected, devoid of intensity oscillations originating in the diatom.

One is concerned, of course, that polarization modulation might degrade the spatial resolution of the microscope. To minimize this possibility, the modulator was placed adjacent to the polarizer, where it was close to the condenser aperture plane and distant from the light-source field plane. To test the resolution, images of the diatom *Pleurosigma angulatum*, which has structural features with a periodicity of about 500 nm, were obtained by polarization-modulated
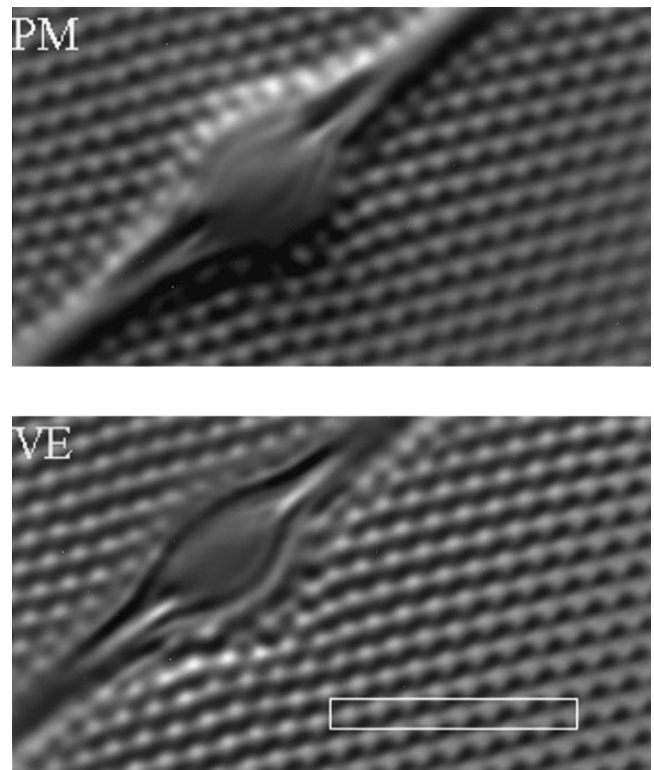


**Fig. 4.** Polarization-modulated DIC image (top) and video-enhanced DIC image (bottom) of the diatom *Pleurosigma angulatum*. The spacing between dots is 530 nm, based upon electron-microscopic measurements. Scale bar = 5 $\mu$m. The polarization-modulated DIC image is the difference between PM$_x$ and PM$_y$. The video-enhanced image is the difference between DIC$_x$ and BKGD.

DIC and by standard video-enhanced DIC. A comparison between the polarization-modulated DIC image and the video-enhanced DIC image (Fig. 4) suggests that the resolution is the same.

### Discussion

One limitation of the present demonstration of polarization-modulated DIC is that alternate images were subtracted off-line because of limitations of available image processing hardware and software. PM-DIC would be more practical if the difference images were immediately visible to the microscopist for ease in focusing and selection of the most interesting features in the sample slide. The key requirement, synchronization of the modulator to the camera, is already achieved. The required frame-rate processing could be implemented on any one of several commercial image acquisition boards with sufficient onboard frame-processing capability. Alternatively, the processing could be done in random-access memory of a sufficiently fast computer.

Once installed, PM-DIC would be simpler than the current VE-DIC procedure, because the microscopist would

not need to obtain a separate background image. The small intensity differences which make up the image would be doubled in PM-DIC. Standard image enhancement techniques, such as averaging and edge enhancement, could of course be applied to the stream of PM-DIC difference images.

The new method does require that the modulator be synchronized with frame acquisition by the camera. Cameras with significant lag, such as newvicons, must be avoided; lag averages out the small intensity differences between alternate frames upon which the method rests.

Polarization-modulation synchronized to frame acquisition might be useful in other modes of microscopy which employ polarized light. For example, by modulating the polarization of the excitation beam in a fluorescence microscope, fluoresence-detected linear dichroism could be used to measure local alignment within single DNA molecules, thereby measuring local tension.

## Conclusions

It has been demonstrated that polarization modulation can improve contrast by a factor of two in video-enhanced DIC microscopy. The required modulator costs less than US$1000 and is small enough to fit easily into a standard DIC microscope. Once installed in a video microscope with frame-rate processing power, the new method should be easier to use than methods which require acquisition and subtraction of a separate background image. Because it is a difference method, PM-DIC can take advantage of the superior dynamic range, low noise, improved precision and faster readout rates of the current generation of scientific-grade CCD detectors.

## Acknowledgments

## References

Allen, R.D. & Allen, N.S. (1983) Video-enhanced microscopy with a computer frame memory. *J. Microsc.* **129**, 3–17.

Allen, R.D., Allen, N.S. & Travis, J.L. (1981) Video-enhanced contrast, differential interference contrast (AVEC-DIC) microscopy. *Cell Motility*, **1**, 291–302.

Allen, R.D., David, G.B. & Nomarski, G.Z. (1969) The Zeiss–Nomarski differential interference equipment for transmitted-light microscopy. *Wiss. Mikrosk. mikroscop. Tech.* **69**, 193–221.

Hansen, E.W., Allen, R.D., Strohbehn, J.W., Chaffee, M.A., Farrington, D.L., Murray, W.F., Pillsbury, T.A. & Riley, M.F. (1985) Laser scanning phase modulation microscope. *J. Microsc.* **140**, 371–381.

Horowitz, P. & Hill, W. (1989) *The Art of Electronics*. Cambridge University Press.

Inoué, S. (1981) Video image processing greatly enhances contrast, quality, and speed in polarization-based microscopy. *J. Cell Biol.* **89**, 346–356.

Inoué, S. (1986) *Video Microscopy*. Plenum Press, New York.

Juang, C.-B., Finzi, L. & Bustamante, C.J. (1988) Design and application of a computer-controlled confocal scanning differential polarization microscope. *Rev. Sci. Instrum.* **59**, 2399–2408.

Lang, W. (1968) *Nomarski Differential Interference-Contrast Microscopy*. Carl Zeiss Informations, Oberkochen.

Mickols, W. & Maestre, M.F. (1988) Scanning differential polarization microscope: its use to image linear and circular differential scattering. *Rev. Sci. Instrum.* **59**, 867–872.

Oldenbourg, R. & Mei, G. (1995) New polarized light microscope with precision universal compensator. *J. Microsc.* **180**, 140–147.

Salmon, E.D. (1995) VE-DIC light microscopy and the discovery of kinesin. *Trends Cell Biol.* **5**, 154–158.